

**Thermal stability of the two-dimensional topological color code**

Razieh Mohseninia\*

*Department of Physics, Sharif University of Technology, P.O. Box 11155-9161, Tehran, Iran*

(Received 15 March 2016; published 8 August 2016)

Thermal stability of the topological color code in the presence of a thermal bath is studied. We study the Lindblad evolution of the observables in the weak-coupling limit of the Born-Markov approximation. The autocorrelation functions of the observables are used as a figure of merit for the thermal stability. We show that all of the observables autocorrelation functions decay exponentially in time. By finding a lower bound of the decay rate, which is a constant independent of the system size, we show that the topological color code is unstable against thermal fluctuations from the bath at finite temperature, even though it is stable at  $T = 0$  against local quantum perturbations.

DOI: [10.1103/PhysRevA.94.022306](https://doi.org/10.1103/PhysRevA.94.022306)**I. INTRODUCTION**

The fragility of the qubits in the presence of decoherence and external noise is the biggest obstacle in realizing a scalable quantum computer. To overcome such problems, quantum error correcting codes have been invented [1–9]. The main idea of the error correcting codes is to encode information in a many particle system; this many particle system plays the role of a stable logical qubit. However, error correcting models are themselves the cause of errors and the error threshold below which one can perform fault tolerant quantum computation is very low [10,11].

Topological quantum codes have emerged as the most promising candidates to achieve fault tolerant quantum computation. In these models information is stored in global properties of the model, say topologically degenerate ground states of the system. In particular, this kind of coding is shown to be robust against local perturbations from the environment provided they are local in space and time and they occur at  $T = 0$  temperature. Examples of good topological codes are Kitaev code [12] and topological color code (TCC) [13]. A very important figure of merit to assess the goodness of a topological code is the error threshold. When only qubit errors occur, the error threshold for the TCC turns out to match the one by the Kitaev model, namely, 11% [14,15]. However, for more realistic situations when the measurement process is also prone to errors, the TCC threshold is 4.5% [16,17], even better than the one for the Kitaev code, which is 2.9% [18].

Topological color codes have shown very versatile properties for doing fault-tolerant quantum computation. In 2D, a TCC can implement the Clifford group of gates in a transversal way [13]; this implementation of Clifford group with TCC makes quantum teleportation, distillation of entanglement, and dense coding possible in a fully topological manner. Moreover, three-dimensional extensions of TCC can also achieve universal quantum computation [19]. The first realization of this model has been done in [20].

An open problem is to find topological codes resilient to thermal fluctuations from the environment. A first indication that the behavior of topological codes may be different at nonzero temperature was advanced in [14,15], and then it

was confirmed by a rigorous proof in [21,22] within the setting of the dynamics of quantum open systems governed by Lindblad dynamics. It has been shown in [21,22] that the Kitaev model in two spatial dimensions is not a stable memory in the presence of a thermal bath. Interestingly enough, it is possible to stabilize topological codes under thermal noise provided the lattice system can be defined in higher spatial dimensions. Namely, a thermally robust topological quantum memory in  $D = 4$  spatial dimensions can be constructed with the Kitaev code [23], and a fully fledged universal quantum computer robust to thermal noise can be constructed in  $D = 6$  dimensions with topological color codes [24].

In this paper we address the problem of thermal stability of TCC in a two-dimensional lattice, based on a mathematically rigorous analysis of the thermal effects on the model. According to the paper in [25], the color code on a two-dimensional hexagonal lattice can be mapped to two decoupled Kitaev models on two-dimensional triangular lattices by local unitary actions. In the original lattice on which the color code is defined (hexagonal lattice) qubits lie on vertices of the lattice; however, on the mapped model the qubits lie on the edges of the triangular lattices. Although the color code is mapped to two decoupled toric codes, an error applied from the bath on a single qubit of the color code corresponds in the mapped model to errors causing excitations in the two decoupled toric codes, i.e., the two disjointed lattices. This means that the processes of creation of excitations in these two disjointed lattices are not independent from each other; thus, due to the coupling to the bath, these two disjointed toric codes can be correlated. This possibility was not taken into account in the previous works on the stability of Kitaev model and, therefore, by knowing the thermal stability properties of one toric code one cannot gain any information about the thermal stability of the color code, and this problem is not trivial.

The method that we use is similar to the one that is used in [22]. To this end, we study the dynamics of the TCC, weakly interacting with a heat bath in the Born-Markov approximation. The evolution of the observables governed by Lindblad dynamics and their autocorrelation function in time is studied as a tool for proving the instability of this model. We show that all of the observables autocorrelation functions decay exponentially with a constant decay rate which means that the model is unstable against thermal noise, although it is stable against local quantum perturbation at zero temperature.

\*mohseninia@physics.sharif.ir

The rest of the paper is organized as follows. In Sec. II we review the main features of the TCC. In Sec. III we provide some basic results of the Markovian approximation in the weak-coupling limit. Section IV deals with reviewing the stability and instability conditions of the topological memories. In Sec. V these conditions are checked for the case of TCC and its instability is proved rigorously. Finally, Sec. VI is devoted to conclusive remarks. In the Appendix, we prove the negativity of the Lindblad superoperator.

## II. TOPOLOGICAL COLOR CODE

Topological color code is a class of topological codes that can be defined on any three colorable lattice, where by colorable we mean colorable by face or equivalently by edge [13]. In the present work, we consider a two-dimensional hexagonal lattice, 2-colex [26], on which the periodic boundary conditions are imposed on both sides. This lattice consists of  $N$  plaquettes,  $2N$  vertices, and  $3N$  edges. A three colorable lattice is a lattice on which one can color its plaquettes with three different colors (red, green, blue [27]) in a way that the plaquettes with the same color do not share any links. Each link connects two plaquettes with the same color and, therefore, one can ascribe every link with this special color.

The qubits, in this model, live on the vertices. The Hamiltonian of the model consists of two kinds of plaquette operators,  $B_p^x$  and  $B_p^z$ , which are defined as follows:

$$B_p^x = \prod_{i \in p} \sigma_{x,i}, \quad B_p^z = \prod_{i \in p} \sigma_{z,i}, \quad (1)$$

where  $\sigma_x$  and  $\sigma_z$  are ordinary Pauli operators and  $p$  denotes a plaquette. Note that  $B_p^x$  and  $B_p^z$  can be defined for all the plaquettes and thus we have a total of  $N$  distinct  $B_p^x$  operators and  $N$  distinct  $B_p^z$  operators. The Hamiltonian is given by

$$H = -J \sum_p B_p^x - J \sum_p B_p^z, \quad (2)$$

where the summation is done over all of the plaquettes. All of the operators in the Hamiltonian commute with each other, since they either share two qubits or none. Thus the Hamiltonian is exactly solvable. The plaquette operators also square to identity and, therefore, have  $\pm 1$  eigenvalues.

One should note that there are  $2N$  qubits and  $2N$  stabilizers [28] (for further details about stabilizer quantum codes, please see [29,30]) in the Hamiltonian. Nevertheless, all of these stabilizers are not independent, because of these constraints on the torus:

$$\prod_{p \in R} B_p^\sigma = \prod_{p \in B} B_p^\sigma = \prod_{p \in G} B_p^\sigma, \quad \sigma = x, z. \quad (3)$$

The number of constraints for each type of plaquette operators ( $\{B_p^x\}$  and  $\{B_p^z\}$ ) is 2; therefore, there are  $2N - 4$  independent stabilizers in the Hamiltonian and the Hamiltonian has  $\frac{2^{2N}}{2^{2N-4}} = 16$  degenerate ground states. The ground subspace of the Hamiltonian is the subspace spanned by the states which are stabilized by all of the plaquette operators

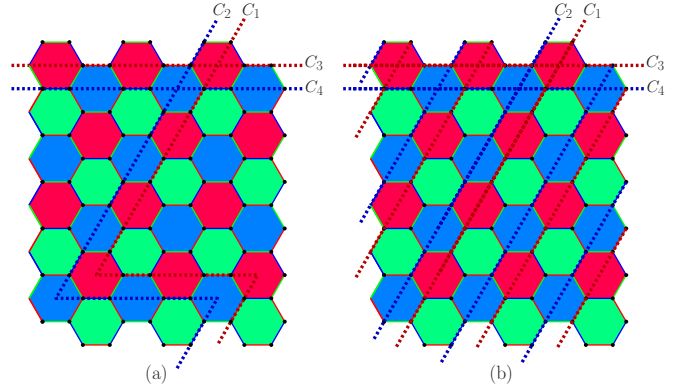


FIG. 1. TCC on a hexagonal lattice. The logical operators are defined on nontrivial loops shown with  $C_i$ 's. (a) The nontrivial loops  $C_1$  and  $C_2$  turn around the torus once. (b) The nontrivial loops  $C_1$  and  $C_2$  turn around the torus three times and they pass all of the plaquettes having the same color.

simultaneously ( $B_p^x |gs\rangle = B_p^z |gs\rangle = |gs\rangle$ ) and one of these states can be represented as

$$|gs\rangle = \prod_p (1 + B_p^x) |0\rangle^{\otimes N}, \quad (4)$$

up to a normalization factor. To construct the other 15 ground states one needs to define the following logical operators:

$$Z_1 = \prod_{i \in C_1} \sigma_{z,i}, \quad Z_2 = \prod_{i \in C_2} \sigma_{z,i},$$

$$Z_3 = \prod_{i \in C_3} \sigma_{z,i}, \quad Z_4 = \prod_{i \in C_4} \sigma_{z,i}, \quad (5)$$

$$X_1 = \prod_{i \in C_4} \sigma_{x,i}, \quad X_2 = \prod_{i \in C_3} \sigma_{x,i},$$

$$X_3 = \prod_{i \in C_2} \sigma_{x,i}, \quad X_4 = \prod_{i \in C_1} \sigma_{x,i}, \quad (6)$$

where  $C_1, C_2, C_3,$  and  $C_4$  are four nontrivial loops in the torus in the sense that they cannot be written as a tensor product of some plaquette operators (Fig. 1). One should note that there are only two nontrivial loops for each nontrivial homology cycles in a torus, the blue loop and the red loop; the third nontrivial loop (green) can be written as a tensor product of the red and the blue ones, i.e.,

$$C_r C_b C_g \sim 1, \quad C_r C_b \sim C_g, \quad (7)$$

up to some plaquette operators. Using these logical operators, all of the 16 ground states can be represented as follows:

$$|i_1, i_2, i_3, i_4\rangle = X_1^{i_1} X_2^{i_2} X_3^{i_3} X_4^{i_4} |gs\rangle, \quad i_n = 0, 1, n = 1, 2, 3, 4. \quad (8)$$

The nontrivial loops can be represented in two ways as shown in Fig. 1. In Fig. 1(a) they turn around the torus once, while in Fig. 1(b) they turn around three times (which is a function of the system size). One should note that the two types of representing the loops are equivalent in the sense that one can deform the two representations into each other by using a set

of appropriate plaquette operators. The second representation [Fig. 1(b)] will be used in Sec. V.

In a realization of topological color code, information can be stored in the topologically degenerate ground states of the system. One can use the ground states to encode four logical qubits. Due to its topological order, the model is robust against local perturbations and the only perturbations that may cause logical error are those with a length equal to the system size. Moreover, the Clifford group's generators can be implemented by this model, which is sufficient for doing quantum distillation of entanglement without any need to address single qubits and to braid the quasiparticles [13,19].

### III. MARKOVIAN APPROXIMATION IN THE WEAK-COUPLING LIMIT

Consider a quantum system which is not closed and is coupled to a thermal bath at temperature  $T$ . One can attribute the following total Hamiltonian to the system and the bath, which form a closed system together:

$$H = H^{\text{sys}} + H^{\text{bath}} + H^{\text{int}}, \quad H^{\text{int}} = \sum_{\alpha} S_{\alpha} \otimes f_{\alpha}, \quad (9)$$

where  $H^{\text{sys}}$  is the topologically ordered Hamiltonian of the system whose stability is being studied and  $H^{\text{bath}}$  is the Hamiltonian of the bath of which we do not have any knowledge and  $H^{\text{int}}$  is the system-bath interaction Hamiltonian.  $S_{\alpha}$ 's are operators acting on the system and  $f_{\alpha}$ 's are operators acting on the bath, and without loss of generality we can assume that they are Hermitian [31].

In the weak-coupling limit of the interaction Hamiltonian, an operator in the Heisenberg picture evolves as follows [31–34]:

$$\frac{dX}{dt} = \mathcal{G}(X) := i[H^{\text{sys}}, X] + \mathcal{L}(X), \quad (10)$$

where  $i$  is the complex imaginary unit and  $\mathcal{G}$  is the generator of the evolution, which consists of two parts. The first part is the normal generator of the evolution of closed quantum systems and the second one is the Lindblad generator or the dissipative part of the evolution, due to existence of the bath. The latter can be given as [31–34]

$$\begin{aligned} \mathcal{L}(X) &= \sum_{\alpha} \sum_{\omega \geq 0} \mathcal{L}_{\alpha, \omega}(X) \\ &= \frac{1}{2} \sum_{\alpha} \sum_{\omega \geq 0} h_{\alpha}(\omega) (S_{\alpha}^{\dagger}(\omega) [X, S_{\alpha}(\omega)] + [S_{\alpha}^{\dagger}(\omega), X] S_{\alpha}(\omega) \\ &\quad + e^{-\beta\omega} S_{\alpha}(\omega) [X, S_{\alpha}^{\dagger}(\omega)] + e^{-\beta\omega} [S_{\alpha}(\omega), X] S_{\alpha}^{\dagger}(\omega)), \end{aligned} \quad (11)$$

where  $\beta$  is the inverse of the temperature of the system and the factors  $h_{\alpha}(\omega)$ 's are the Fourier transforms of the autocorrelation functions of  $f_{\alpha}$ 's and we have used the relations  $h_{\alpha}(-\omega) = e^{-\beta\omega} h_{\alpha}(\omega)$ . In addition,  $S_{\alpha}(\omega)$  is the Fourier transform of  $S_{\alpha}$ :

$$S_{\alpha}(\omega) = \sum_{\epsilon = -\epsilon' = \omega} \Pi_{\epsilon'} S_{\alpha} \Pi_{\epsilon}, \quad (12)$$

where  $\Pi_{\epsilon}$  is the projector onto the subspace with energy  $\epsilon$  and  $\omega$ 's are the Bohr frequencies of the system Hamiltonian. One can further check that  $S_{\alpha}(-\omega) = S_{\alpha}^{\dagger}(\omega)$  and  $\sum_{\omega} S_{\alpha}(\omega) = S_{\alpha}$ .

#### Properties of the Lindblad superoperator

In this section we briefly review some of the essential features of the Lindblad superoperator needed for our study.

(i) *Self-adjointness of  $\mathcal{L}$* . If we define the Liouville scalar product as follows:

$$\langle X, Y \rangle_{\beta} := \text{tr}(\rho_{\beta} X^{\dagger} Y), \quad (13)$$

the Lindblad superoperator is self-adjoint with respect to it, i.e.,

$$\langle X, \mathcal{L}(Y) \rangle_{\beta} = \langle \mathcal{L}(X), Y \rangle_{\beta}. \quad (14)$$

From here on, in the rest of this paper by scalar product we mean the Liouville scalar product and we withdraw writing  $\beta$  symbol.

(ii) *Positivity of  $-\mathcal{L}$* . The Lindblad superoperator is negative which means that

$$-\langle X, \mathcal{L}(X) \rangle \geq 0, \quad \forall X. \quad (15)$$

The negativity of  $\mathcal{L}$  is proved in the Appendix.

(iii) *Gap of  $-\mathcal{L}$* . Because of the positivity of  $-\mathcal{L}$ , its smallest eigenvalue different from zero is defined as its gap:

$$G(-\mathcal{L}) := \min_X (-\langle X, \mathcal{L}(X) \rangle : \forall X \neq I). \quad (16)$$

where  $I$  is the identity operator.

### IV. STABILITY AND INSTABILITY CONDITIONS FOR TOPOLOGICAL MEMORIES

(i) *Stability*. To prove the stability of a memory at finite temperature and its capability for coding the information, one should find an observable as the logical operator for the logical qubit such that by increasing the system size the autocorrelation function of the observable does not decrease in time. More rigorously one should find an observable  $X$  and a decay rate  $\epsilon$ , such that

$$\langle X, X(t) \rangle \geq e^{-\epsilon t} \langle X, X \rangle, \quad (17)$$

where  $\epsilon$  is the decay rate of the autocorrelation function of the observable  $X$ . In the case of a stable memory the decay rate should decrease exponentially with system size ( $\epsilon = e^{-N^a}$ ), so that by increasing the system size the decay rate goes to zero. This means that the autocorrelation function of an observable, in the limit of large system size, will not decrease in time and the memory will be stable and self-correcting [23]. By substituting  $X(t) = e^{t\mathcal{L}} X$  into Eq. (17), the condition for the stability recasts into the following:

$$-\langle X, \mathcal{L}(X) \rangle \leq \epsilon, \quad (18)$$

where  $\epsilon$  decays exponentially with the system size.

(ii) *Instability*. To prove the instability of a memory one should prove that the autocorrelation function of all of the observables with time decreases faster than an exponential function, which means that for any observable

we have

$$\langle X, X(t) \rangle \leq e^{-\epsilon t} \langle X, X \rangle. \quad (19)$$

By substituting  $X(t) = e^{t\mathcal{L}}X$  into the above equation the instability condition of a memory recasts into the following:

$$-\langle X, \mathcal{L}(X) \rangle \geq \epsilon, \quad (20)$$

which means that for proving the instability of a memory one should estimate a lower bound of  $-\langle X, \mathcal{L}(X) \rangle$  by minimizing it over all of the observables. If this quantity is a constant independent of the system size or is a variable of the system size that does not decrease with the size of the system, the memory is unstable, since in finite time the autocorrelation goes to zero and the encoded information lost (for more details, please see [22,35]).

Therefore, proving the instability of a memory is nothing but obtaining the gap of  $-\mathcal{L}$ , which is denoted by  $G$ :

$$G(-\mathcal{L}) := G = \min_X (-\langle X, \mathcal{L}(X) \rangle : \forall X \neq I). \quad (21)$$

Applying Eq. (A4) (see the Appendix for further details), one obtains

$$G \geq \frac{1}{2} \min_{\alpha, \omega} [h_\alpha(\omega)] \min_X \left( \sum_{\alpha, \omega} \langle [S_\alpha(\omega), X], [S_\alpha(\omega), X] \rangle \right). \quad (22)$$

Moreover, by using Eq. (28) of Ref. [23] which indicates that

$$\sum_{\omega} \langle [S_\alpha(\omega), X], [S_\alpha(\omega), X] \rangle = \sum_{\omega, \omega'} \langle [S_\alpha(\omega), X], [S_\alpha(\omega'), X] \rangle \quad (23)$$

and the relation  $\sum_{\omega} S_\alpha(\omega) = S_\alpha$ , we obtain

$$G \geq \frac{1}{2} \min_{\alpha, \omega} (h_\alpha(\omega)) \min_X \left( \sum_{\alpha} \langle [S_\alpha, X], [S_\alpha, X] \rangle \right), \quad (24)$$

which is easier to estimate. One should note that  $h_\alpha(\omega)$  is the Fourier transform of the autocorrelation function of  $f_\alpha$  and it can be supposed that  $h_\alpha(\omega)$  does not depend on  $\alpha$ 's, which means that the action of the bath and the strength of interaction Hamiltonian is uniform in the whole system. Thus the minimum of  $h_\alpha(\omega)$  is equal to  $e^{-\beta\Delta}h(\Delta)$ , where  $\Delta$  is the gap of the Hamiltonian and, for TCC,  $\Delta$  is equal to  $6J$ . Therefore, the lower bound of the gap recasts into the following:

$$G \geq \frac{1}{2} e^{-\beta\Delta} h(\Delta) \min_X \left( \sum_{\alpha} \langle [S_\alpha, X], [S_\alpha, X] \rangle \right). \quad (25)$$

## V. THERMAL INSTABILITY OF THE TOPOLOGICAL COLOR CODE

Consider a realization of the topological color code, which is coupled to a thermal bath at temperature  $T$ . Due to this coupling, errors can be applied from the bath on the system. The errors usually do not commute with the Hamiltonian and the system will not remain in the ground states anymore. If the system is able to correct itself, i.e., it can remove errors to stay in the ground subspace, it can be considered as a stable topological memory.

In the present work, thermal stability of TCC at finite temperature is studied. We assume that the interaction Hamiltonian between the system and the bath is of the following form:

$$H^{\text{int}} = \sum_i (\sigma_{x,i} \otimes f_{x,i} + \sigma_{z,i} \otimes f_{z,i}), \quad (26)$$

where  $\sigma_x$  and  $\sigma_z$  are applied from the bath on each qubit. To understand the effect of this Hamiltonian on the system, consider the  $i$ th qubit, for example;  $\sigma_{x,i}$  ( $\sigma_{z,i}$ ) anticommutes with the three  $z$  type ( $x$  type) plaquette operators that have this qubit in common. Thus, if  $\sigma_{x,i}$  acts from the bath on the ground state, because of this anticommutation, the eigenvalues of the three plaquettes operators become  $-1$  and the system leaves the ground subspace and consequently the code space.

We can assume that in a plaquette with  $-1$  eigenvalue, an excitation (quasiparticle) has been created. In TCC the excitations can move freely and cause logical errors. Therefore, it seems that the model is not self-correcting. By having this intuition we present a rigorous proof of the instability of this model, i.e., we shall estimate a lower bound for the gap of the Lindblad superoperator corresponding to the model as it is discussed in the previous section.

### A. Excitations

If the operators that are applied from the bath on the system do not commute with the Hamiltonian, they create excitations. In this section we introduce the generators for having all possible excitations in TCC. In this model the excitations appear in many different ways and not necessarily in pairs; however, all of them can be generated by the use of the following two kinds of generators.

(i) *Open strings*. Corresponding to each color, there is a global open string as shown in Fig. 2(b). The red global open string, for example, is obtained by inserting a site at the center of every red plaquette and then connecting the sites through the red links which have the same orientation [36] [exactly as the  $C_r$  string shown in Fig. 2(b)]. Note that each link of the global strings corresponds to two nearest neighbor qubits in the original lattice. Let us refer to the connected subsets of the global open strings as open strings.

As an example, consider an open string with only one link. By acting with  $\sigma_x \otimes \sigma_x$  or  $\sigma_z \otimes \sigma_z$  on the two qubits that lie

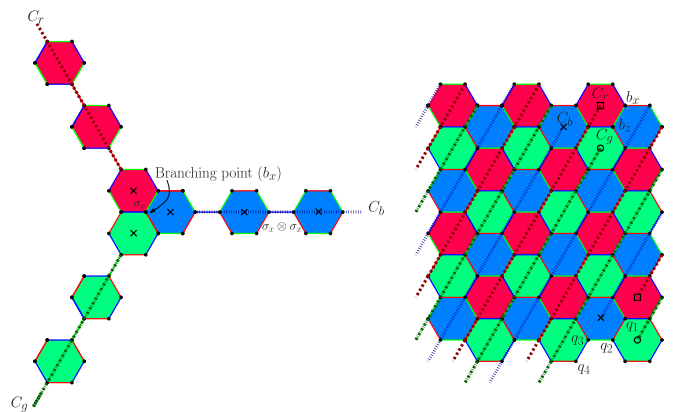


FIG. 2. Open strings  $C_r, C_b, C_g$  and branching points  $b_x, b_z$  for creating all kinds of excitations in TCC.

on the only link of the string, the two plaquettes that are on the two ends of the string will be excited [Fig. 2(a)]. By increasing the length of this string one can move the excitations to any other two red plaquettes.

In this case, excitations appear in pairs. In a lattice with  $N$  plaquettes and  $2N$  qubits, to generate all of the open string operators,  $2N - 6$  qubits are needed; these qubits are located on  $C_r$ ,  $C_b$ , and  $C_g$  global strings.

(ii) *Branching points.* In TCC it is possible to have three excitations in three plaquettes with different colors. It is impossible to create such excitations by using the open strings; however, by using a single-qubit operator along with the open string operators, one can have all kinds of excitations. More rigorously, by acting with  $\sigma_x$  on one qubit, which we call branching point, excitations are created in the three plaquettes that have this qubit in common [37]. By using open strings one can move the excitations from these three plaquettes to other plaquettes with the same color.

One should note that because of the relation (3), an arbitrary number of excitations for different colors are not allowed and there are certain constraints on the number of excitations of different colors. For example, a single excitation with red color is not allowed.

Therefore, all kinds of excitations can be generated by applying  $\sigma_x \otimes \sigma_x$  or  $\sigma_z \otimes \sigma_z$  on the qubits that belong to the open strings and also  $\sigma_x$  and  $\sigma_z$  on the branching points  $b_x$  and  $b_z$ , respectively.

In a hexagonal lattice with  $2N$  qubits, to generate all kinds of excitations one needs  $2N - 6 + 2 = 2N - 4$  qubits. Thus four qubits are left [ $q_1$ ,  $q_2$ ,  $q_3$ , and  $q_4$  shown in Fig. 2(b)]. This is consistent with having 16 degenerate ground states and 4 logical qubits.

### B. Observables

All of the observables corresponding to a two-dimensional Hilbert space can be generated by  $\sigma_x$  and  $\sigma_z$ . Therefore, the algebra of the observables for a system consisting of  $N$  qubits may be written as

$$\mathcal{O} = \mathcal{Q}_1 \otimes \mathcal{Q}_2 \otimes \cdots \otimes \mathcal{Q}_N, \quad (27)$$

where  $\mathcal{Q}_i$  is the algebra of the observables of the  $i$ th qubit which is generated by  $\sigma_{x,i}$  and  $\sigma_{z,i}$ . However, one can construct all of the observables in another way by the use of the operators present in the Hamiltonian, the logical operators and the generators needed to create all kinds of excitations. The latter depends on the form of the Hamiltonian. For the case of TCC, the generators of the algebra of the observable are of the following three types.

(i) The  $x$  and  $z$  type plaquette operators in the Hamiltonian,  $B_p^x$ ,  $B_p^z$  operators.

(ii) The logical operators defined in Eqs. (5) and (6) [38].

(iii) The generators of the excitations:  $\sigma_x \otimes \sigma_x$  or  $\sigma_z \otimes \sigma_z$  acting on two nearest-neighbor qubits that lie on  $C_r$ ,  $C_b$ , and  $C_g$  strings (Fig. 2);  $\sigma_x$  acting on  $b_x$  and  $\sigma_z$  acting on  $b_z$ .

### C. Gap of generator of the topological color code

In this section, to prove the thermal instability of the TCC, we obtain a lower bound for the gap of generator of the

evolution, due to the coupling to the thermal bath, and show that it is a constant independent of the system size. To this end we refer to Eq. (25) which for the interaction Hamiltonian defined in Eq. (26) recasts into the following form:

$$G \geq \frac{1}{2} e^{-\beta \Delta} h(\Delta) \min_{\Gamma} \left( \sum_i \langle [\sigma_{x,i}, \Gamma], [\sigma_{x,i}, \Gamma] \rangle + \langle [\sigma_{z,i}, \Gamma], [\sigma_{z,i}, \Gamma] \rangle \right). \quad (28)$$

The minimization in Eq. (28) is performed over all of the observables. However, if one wants an observable to be a logical observable acting on the code space, it should commute with the Hamiltonian. Therefore, we do not need to do the minimization over all of the observables on Hilbert space explained in the previous section; the observables that commute with the Hamiltonian would suffice. One can restrict the domain of the minimization even more; the logical observables  $Z$  and  $X$  for one logical qubit should anticommute and square to identity. Therefore, all of the observables of our interest belong to the following algebra:

$$\mathcal{O} = (Z_1^{\mu_1} X_1^{\nu_1})(Z_2^{\mu_2} X_2^{\nu_2})(Z_3^{\mu_3} X_3^{\nu_3})(Z_4^{\mu_4} X_4^{\nu_4})(B_p^z \otimes B_p^x), \quad \mu_i = 0, 1 \quad \text{and} \quad \nu_i = 0, 1, \quad (29)$$

where  $B_p^z$  and  $B_p^x$  are the algebras generated by all of the  $z$  and  $x$  type plaquette operators, respectively, and the minimization is over different possibilities of  $\mu_i$ 's and  $\nu_i$ 's and also the two algebras  $B_p^z$  and  $B_p^x$ . By putting an observable  $\Gamma \in \mathcal{O}$  (some observable of our interest) into Eq. (28), one finds that

$$G \geq \frac{1}{2} e^{-\beta \Delta} h(\Delta) \left( \min_{\Gamma_z} \left( \sum_i \langle [\sigma_{x,i}, \Gamma_z], [\sigma_{x,i}, \Gamma_z] \rangle \right) + \min_{\Gamma_x} \left( \sum_i \langle [\sigma_{z,i}, \Gamma_x], [\sigma_{z,i}, \Gamma_x] \rangle \right) \right). \quad (30)$$

Here by  $\Gamma_z$  and  $\Gamma_x$  we mean operators belonging to the following subalgebras, respectively:

$$\mathcal{O}_{\ddagger} = (Z_1^{\mu_1} Z_2^{\mu_2} Z_3^{\mu_3} Z_4^{\mu_4}) B_p^z, \quad (31)$$

$$\mathcal{O}_{\S} = (X_1^{\nu_1} X_2^{\nu_2} X_3^{\nu_3} X_4^{\nu_4}) B_p^x. \quad (32)$$

Therefore, we have

$$G \geq \frac{1}{2} (g_x + g_z), \quad (33)$$

where  $g_x$  ( $g_z$ ) comes from  $\sigma_x$  ( $\sigma_z$ ) part of the interaction Hamiltonian:

$$g_x = e^{-\beta \Delta} h(\Delta) \min_{\Gamma_z} \left( \sum_i \langle [\sigma_{x,i}, \Gamma_z], [\sigma_{x,i}, \Gamma_z] \rangle \right), \quad (34)$$

$$g_z = e^{-\beta \Delta} h(\Delta) \min_{\Gamma_x} \left( \sum_i \langle [\sigma_{z,i}, \Gamma_x], [\sigma_{z,i}, \Gamma_x] \rangle \right). \quad (35)$$

By symmetry we know that  $g_x$  and  $g_z$  are equal to each other. Thus the lower bound of the gap reduces to  $G \geq g_x$ , i.e.,

$$G \geq e^{-\beta\Delta} h(\Delta) \min_{\Gamma_z} \left( \sum_i \langle [\sigma_{x,i}, \Gamma_z], [\sigma_{x,i}, \Gamma_z] \rangle \right). \quad (36)$$

To obtain a lower bound of the gap, one can partition the algebra of all of the observables into different sectors (different possibilities of  $\mu_i$ 's) and obtain a lower bound for each sector and, at the end, perform the minimization over all of the sectors.

### 1. Sector of $\Gamma_z = Z_1 \mathcal{B}_p^z$ or $\Gamma_z = Z_2 \mathcal{B}_p^z$

Let us show the minimum of the decay rate in this sector by  $G_1$ . By symmetry, we know that the effect of the external bath on  $Z_1 \mathcal{B}_p^z$  is exactly the same as its effect on  $Z_2 \mathcal{B}_p^z$ . Thus it is enough to consider only one of them, say  $Z_1 \mathcal{B}_p^z$ :

$$G_1 \geq e^{-\beta\Delta} h(\Delta) \min_{\Gamma_z} \left( \sum_i \langle [\sigma_{x,i}, Z_1 \mathcal{B}_p^z], [\sigma_{x,i}, Z_1 \mathcal{B}_p^z] \rangle \right). \quad (37)$$

From now on, we use the notation used in [22], and show the terms  $\langle [\sigma_{x,i}, Z_1 \mathcal{B}_p^z], [\sigma_{x,i}, Z_1 \mathcal{B}_p^z] \rangle$  as  $\mathcal{L}_{x,i}^1$  for example. Therefore, we have

$$\begin{aligned} & \sum_i \langle [\sigma_{x,i}, Z_1 \mathcal{B}_p^z], [\sigma_{x,i}, Z_1 \mathcal{B}_p^z] \rangle \\ &= \sum_i \mathcal{L}_{x,i}^1 = \mathcal{L}_{x,q_1}^1 + \mathcal{L}_{x,q_2}^1 + \mathcal{L}_{x,q_3}^1 + \mathcal{L}_{x,q_4}^1 + \mathcal{L}_{x,b_x}^1 \\ & \quad + \mathcal{L}_{x,b_z}^1 + \mathcal{L}_{x,C_b}^1 + \mathcal{L}_{x,C_g}^1 + \mathcal{L}_{x,C_r}^1 \\ & \geq \mathcal{L}_{x,C_b}^1 + \mathcal{L}_{x,C_g}^1 + \mathcal{L}_{x,C_r}^1, \end{aligned} \quad (38)$$

where by  $\mathcal{L}_{x,C_b}^1$  we mean  $\sum_{i \in C_b} \mathcal{L}_{x,i}^1$  and so on. To obtain the inequality in Eq. (38), we have used the positivity of each term  $\mathcal{L}_{x,i}^1$ , which is proved in the Appendix. Now we calculate the terms  $\mathcal{L}_{x,C_b}$ ,  $\mathcal{L}_{x,C_g}$ , and  $\mathcal{L}_{x,C_r}$  separately as follows:

$$\begin{aligned} \mathcal{L}_{x,C_b}^1 &= \sum_{i \in C_b} \langle [\sigma_{x,i}, Z_1 \mathcal{B}_p^z], [\sigma_{x,i}, Z_1 \mathcal{B}_p^z] \rangle \\ &= \sum_{i \in C_b} \langle Z_1 [\sigma_{x,i}, \mathcal{B}_p^z], Z_1 [\sigma_{x,i}, \mathcal{B}_p^z] \rangle \\ &= \sum_{i \in C_b} \text{tr}(\rho_\beta [\sigma_{x,i}, \mathcal{B}_p^z]^\dagger Z_1^\dagger Z_1 [\sigma_{x,i}, \mathcal{B}_p^z]) \\ &= \sum_{i \in C_b} \langle [\sigma_{x,i}, \mathcal{B}_p^z], [\sigma_{x,i}, \mathcal{B}_p^z] \rangle, \end{aligned} \quad (39)$$

where the second line is the consequence of the fact that  $Z_1$  commutes with all of  $\sigma_{x,i}, i \in C_b$  [Fig. 1(b) and Fig. 2(b)], because the support of  $Z_1$  and  $C_b$  do not have any common qubit.

One can further check that the same arguments as above also hold for  $\mathcal{L}_{x,C_g}^1$ . On the contrary, the term  $\mathcal{L}_{x,C_r}^1$  leads to a different result, since the support of  $Z_1$  and  $C_r$  meet each other and, therefore,  $Z_1$  does not commute with  $\sigma_{x,i}$ 's,  $i \in C_r$ . However, as shown in Eq. (7) in TCC a nontrivial loop with a specific color, say red, is equivalent to the tensor product of two other nontrivial loops that have different colors, green and blue, but are in the same homology class as the red one. Therefore, one can write  $Z_1$ , (denoted as  $Z_r$ ) as the tensor product of  $Z_2$  (denoted as  $Z_b$ ) and another logical operator that is defined on a green nontrivial loop (denoted as  $Z_g$ ), i.e.,

$$Z_r Z_b Z_g \sim 1, \quad Z_r \sim Z_g Z_b, \quad (40)$$

up to some plaquette operators. Thus

$$Z_r \mathcal{B}_p^z = Z_g Z_b \mathcal{B}_p^z, \quad (41)$$

where we have absorbed the extra plaquette operators, in the algebra of all of the plaquette operators. Because  $Z_g Z_b$  does not meet  $C_r$  at any point, the same result as  $\mathcal{L}_{x,C_g,b}^1$  also holds for the last term  $\mathcal{L}_{x,C_r}^1$ . Suppose that  $A$  and  $B$  have their minimum values at  $X_1$  and  $X_2$ , respectively; since  $A + B$  would, in general, have its minimum at  $X_3$  which is different from  $X_1$  and  $X_2$ , one arrives at

$$\min_X (A + B) \geq \min_X (A) + \min_X (B). \quad (42)$$

By using this inequality the lower bound of the gap of Lindblad in this sector recasts into the following:

$$G_1 \geq 3e^{-\beta\Delta} h(\Delta) \min_{\Gamma_z} \mathcal{L}_{x,C_b}^1. \quad (43)$$

Here,  $\Gamma_z \in \mathcal{B}_p^z$ . Obtaining the gap of this new model is simpler, because by knowing the effect of the bath on this new model one can map it to a known model so that its Lindblad gap is known. The new model is nothing but the Ising model. The reason is that in TCC when  $\sigma_x$  is applied on one qubit, say qubit number 1 in Fig. 3(a), it can create three excitations in three plaquettes that have this qubit in common; by acting another  $\sigma_x$  on the next qubit, qubit number 2, two of these excitations will be annihilated and a new one can be created in the next blue plaquette [Fig. 3(a)]. On the other hand, consider another model, one-dimensional Ising model, with inhomogeneous couplings as follows:

$$H_{\text{Ising}} = -J \sum_{i=\text{odd}} \sigma_{z,i} \sigma_{z,i+1} - 2J \sum_{i=\text{even}} \sigma_{z,i} \sigma_{z,i+1}, \quad (44)$$

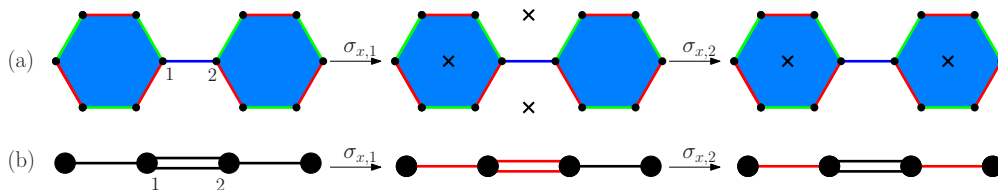


FIG. 3. Equivalence of the process of creation of excitation in the blue sublattice in the TCC, as shown in (a), and the inhomogeneous Ising model, as shown in (b).

where  $J$  is the coupling constant. In this model if  $\sigma_x$  is applied to qubit number 1 in Fig. 3(b), it excites two of the bonds; however since one of the coupling strength is twice the other one, one can suppose that this external perturbation creates three excitations with the same energy [the excited bonds are shown with red color in Fig. 3(b)]. By applying another  $\sigma_x$  on qubit number 2 the bond with two excitations is not excited any more, but another bond with one excitation can be excited. Thus the process of creation and annihilation of excitation in the TCC is exactly what happens in the Ising model defined in Eq. (44). It has been shown in [22] that the Ising model with arbitrary coupling is not a stable memory against thermal fluctuations, since the gap of Lindblad superoperator for this model is a constant independent of the system size. Therefore, one can conclude that for this sector of observables, the minimum of the decay rate is the following constant, which is independent of the system size:

$$G_1 \geq 3e^{-\beta\Delta}h(\Delta)[G(\mathcal{L})]_{\text{Ising}}. \quad (45)$$

### 2. Sector of $\Gamma_z = \mathcal{B}_p^z$

Let us show the minimum of the decay rate in this sector by  $G_2$ :

$$G_2 \geq e^{-\beta\Delta}h(\Delta) \min_{\Gamma_z} \left( \sum_i \langle [\sigma_{x,i}, \mathcal{B}_p^z], [\sigma_{x,i}, \mathcal{B}_p^z] \rangle \right). \quad (46)$$

As in the previous case, the terms like  $\langle [\sigma_{x,i}, \mathcal{B}_p^z], [\sigma_{x,i}, \mathcal{B}_p^z] \rangle$  are shown as  $\mathcal{L}_{x,i}^2$ . Therefore, we have

$$\begin{aligned} & \sum_i \langle [\sigma_{x,i}, \mathcal{B}_p^z], [\sigma_{x,i}, \mathcal{B}_p^z] \rangle \\ &= \sum_i \mathcal{L}_{x,i}^2 = \mathcal{L}_{x,q_1}^2 + \mathcal{L}_{x,q_2}^2 + \mathcal{L}_{x,q_3}^2 + \mathcal{L}_{x,q_4}^2 \\ & \quad + \mathcal{L}_{x,b_x}^2 + \mathcal{L}_{x,b_z}^2 + \mathcal{L}_{x,C_b}^2 + \mathcal{L}_{x,C_g}^2 + \mathcal{L}_{x,C_r}^2 \\ & \geq \mathcal{L}_{x,C_b}^2 + \mathcal{L}_{x,C_g}^2 + \mathcal{L}_{x,C_r}^2. \end{aligned} \quad (47)$$

By symmetry we know that the three terms  $\mathcal{L}_{x,C_b}^2$ ,  $\mathcal{L}_{x,C_g}^2$ , and  $\mathcal{L}_{x,C_r}^2$  are equal to each other. Thus the minimum decay rate recasts into the following form:

$$G_2 \geq 3e^{-\beta\Delta}h(\Delta) \min_{\Gamma_z} \mathcal{L}_{x,C_b}^2, \quad (48)$$

which is exactly what was discussed in the previous section and was equal to the gap of the Lindblad superoperator for the Ising model defined in Eq. (44). Therefore, we have

$$G_2 \geq 3e^{-\beta\Delta}h(\Delta)[G(\mathcal{L})]_{\text{Ising}}. \quad (49)$$

### 3. Sector of $\Gamma_z = Z_3\mathcal{B}_p^z$ or $\Gamma_z = Z_4\mathcal{B}_p^z$

Let us show the minimum of the decay rate in this sector by  $G_3$ . By symmetry we know that the effect of the external bath on  $Z_3\mathcal{B}_p^z$  is exactly the same as the effect of the bath on  $Z_4\mathcal{B}_p^z$ . Therefore, it is enough to consider only one of them, say  $Z_3\mathcal{B}_p^z$ :

$$G_3 \geq e^{-\beta\Delta}h(\Delta) \min_{\Gamma_z} \left( \sum_i \langle [\sigma_{x,i}, Z_3\mathcal{B}_p^z], [\sigma_{x,i}, Z_3\mathcal{B}_p^z] \rangle \right). \quad (50)$$

In this sector the terms like  $\langle [\sigma_{x,i}, Z_3\mathcal{B}_p^z], [\sigma_{x,i}, Z_3\mathcal{B}_p^z] \rangle$  are represented by  $\mathcal{L}_{x,i}^3$ . Therefore, we have

$$\begin{aligned} G_3 & \geq e^{-\beta\Delta}h(\Delta) \min_{\Gamma_z} \sum_i \mathcal{L}_{x,i}^3 \\ &= e^{-\beta\Delta}h(\Delta) \min_{\Gamma_z} (\mathcal{L}_{x,q_1}^3 + \mathcal{L}_{x,q_2}^3 + \mathcal{L}_{x,q_3}^3 + \mathcal{L}_{x,q_4}^3 \\ & \quad + \mathcal{L}_{x,b_x}^3 + \mathcal{L}_{x,b_z}^3 + \mathcal{L}_{x,C_b}^3 + \mathcal{L}_{x,C_g}^3 + \mathcal{L}_{x,C_r}^3) \\ & \geq e^{-\beta\Delta}h(\Delta) \min_{\Gamma_z} (\mathcal{L}_{x,C_b}^3 + \mathcal{L}_{x,C_g}^3 + \mathcal{L}_{x,C_r}^3) \\ & \geq e^{-\beta\Delta}h(\Delta) (\min_{\Gamma_z} (\mathcal{L}_{x,C_b}^3) + \min_{\Gamma_z} (\mathcal{L}_{x,C_g}^3) + \min_{\Gamma_z} (\mathcal{L}_{x,C_r}^3)). \end{aligned} \quad (51)$$

Now we calculate the terms separately as follows:

$$\min_{\Gamma_z} \mathcal{L}_{x,C_r}^3 = \min_{\Gamma_z} \left( \sum_{i \in C_r} \langle [\sigma_{x,i}, Z_3\mathcal{B}_p^z], [\sigma_{x,i}, Z_3\mathcal{B}_p^z] \rangle \right). \quad (52)$$

Since  $Z_3$ 's support is the closed red string and  $C_r$  is also a red string, in the other homological class, they do not meet each other at any point. Thus  $Z_3$  and  $\sigma_{x,i}$ ,  $i \in C_r$  commute with each other and the above equation reduces to

$$\min_{\Gamma_z} \mathcal{L}_{x,C_r}^3 = \min_{\Gamma_z} \left( \sum_{i \in C_r} \langle [\sigma_{x,i}, \mathcal{B}_p^z], [\sigma_{x,i}, \mathcal{B}_p^z] \rangle \right), \quad (53)$$

which is exactly what was discussed in the first case, and is equal to the gap of the Lindblad superoperator for the Ising model defined in Eq. (44). The only quantities left to be obtained are  $\mathcal{L}_{x,C_b}$  and  $\mathcal{L}_{x,C_g}$ , which by symmetry we know to be equal to each other. Thus it is sufficient to consider only one of them:

$$\min_{\Gamma_z} \mathcal{L}_{x,C_b}^3 = \min_{\Gamma_z} \left( \sum_{i \in C_b} \langle [\sigma_{x,i}, Z_3\mathcal{B}_p^z], [\sigma_{x,i}, Z_3\mathcal{B}_p^z] \rangle \right). \quad (54)$$

We can split the summation  $\sum_{i \in C_b}$  in two parts, the qubits that lie on  $Z_3$  loop and the qubits that do not lie on  $Z_3$  loop:

$$\begin{aligned} \mathcal{L}_{x,C_b}^3 &= \left( \sum_{i \in C_b, i \notin Z_3} \langle [\sigma_{x,i}, Z_3\mathcal{B}_p^z], [\sigma_{x,i}, Z_3\mathcal{B}_p^z] \rangle \right) \\ & \quad + \left( \sum_{i \in C_b, i \in Z_3} \langle [\sigma_{x,i}, Z_3\mathcal{B}_p^z], [\sigma_{x,i}, Z_3\mathcal{B}_p^z] \rangle \right). \end{aligned} \quad (55)$$

We use Lemma 2 in [22] which indicates that a lower bound of the gap of a superoperator like  $\mathcal{S}$  that can be written as summation of two other superoperators, i.e.,  $\mathcal{S} = \mathcal{A} + \mathcal{B}$ , is given by

$$G(\mathcal{S}) \geq \frac{G(\mathcal{A})\langle \ker(\mathcal{A}), \mathcal{B}[\ker(\mathcal{A})] \rangle}{G(\mathcal{A}) + \|\mathcal{B}\|}. \quad (56)$$

We take  $\mathcal{A}$  and  $\mathcal{B}$  to be the Lindblad superoperator when the bath does not have any effect on the qubits lying on  $C_3$  and when the bath is applied only on the qubits lying on

$C_3$ , respectively and  $\ker(\mathcal{A})$  refers to an operator  $\hat{O}$  such that  $\mathcal{A}(\hat{O}) = 0$ . Therefore, for the gap of  $\mathcal{A}$  we have

$$\begin{aligned} G(\mathcal{A}) &= \min_{\Gamma_z} \left( \sum_{i \in C_b, i \notin Z_3} \langle [\sigma_{x,i}, Z_3 \mathcal{B}_p^z], [\sigma_{x,i}, Z_3 \mathcal{B}_p^z] \rangle \right) \\ &= \min_{\Gamma_z} \left( \sum_{i \in C_b, i \notin Z_3} \langle [\sigma_{x,i}, \mathcal{B}_p^z], [\sigma_{x,i}, \mathcal{B}_p^z] \rangle \right). \end{aligned} \quad (57)$$

One should note that the expression in the second line is not the gap of the Ising model, because perturbations from the bath are not applied to all of the qubits lying on  $C_3$ . Nevertheless, one can see that it is the gap of a one-dimensional Ising model whose qubits are missing at some of the points. The number of these points is  $\frac{|C|}{2}$ , where  $|C|$  is the length of  $C_3$  defined as the number of qubits that lie on  $C_3$  loop. Note that there are  $\frac{|C|}{2}$  distinct blue sublattices in between every two adjacent missing points. Therefore, using inequality (42), one can expand  $G(\mathcal{A})$ , as a summation of  $\frac{|C|}{2}$  terms, where each term is equal to the minimum of the decay rate for each of these  $\frac{|C|}{2}$  Ising models that are defined on one of the  $\frac{|C|}{2}$  aforementioned sublattices. Because the minimum of the decay rate for these  $\frac{|C|}{2}$  Ising models are equal to each other, therefore one obtains

$$\begin{aligned} G(\mathcal{A}) &\geq \frac{|C|}{2} \min_{\Gamma_z} \left( \sum_{i \in C_b^1, i \notin Z_3} \langle [\sigma_{x,i}, \mathcal{B}_p^z], [\sigma_{x,i}, \mathcal{B}_p^z] \rangle \right) \\ &\geq 0, \end{aligned} \quad (58)$$

where, by  $C_b^1$ , we mean that the bath is applying on qubits that lie on one of these  $\frac{|C|}{2}$  blue sublattices. The reason that the lower bound for the gap of one of these Ising models is zero is that one can find an observable belonging to  $\mathcal{B}_p^z$ , such that the support of this observable does not have any point in common with the vertices of one of these  $\frac{|C|}{2}$  blue sublattices.

Therefore, from Eqs. (56)–(58), one finds the following lower bound for the gap of  $\mathcal{L}_{x,C_b}^3$  in the present sector:

$$\mathcal{L}_{x,C_b}^3 = \mathcal{L}_{x,C_g}^3 \geq 0. \quad (59)$$

Using Eqs. (51)–(59), the minimum of the decay rate for this sector is given by

$$G_3 \geq \mathcal{L}_{x,C_r}^3 + \mathcal{L}_{x,C_b}^3 + \mathcal{L}_{x,C_g}^3 \geq e^{-\beta\Delta} h(\Delta) G_{\text{Ising}}. \quad (60)$$

#### 4. Sector of $\Gamma_z = Z_1 Z_3 \mathcal{B}_p^z$ or $\Gamma_z = Z_1 Z_4 \mathcal{B}_p^z$ or $\Gamma_z = Z_2 Z_3 \mathcal{B}_p^z$ or $\Gamma_z = Z_2 Z_4 \mathcal{B}_p^z$

The minimum of the decay rate in this sector is shown by  $G_4$ . Using the inequality (42) and the notation  $\mathcal{L}_{C_b,g,r}^4 = \sum_{i \in C_b,g,r} \langle [\sigma_{x,i}, Z_1 Z_3 \mathcal{B}_p^z], [\sigma_{x,i}, Z_1 Z_3 \mathcal{B}_p^z] \rangle$  we obtain

$$\begin{aligned} G_4 &\geq e^{-\beta\Delta} h(\Delta) \left( \min_{\Gamma_z} (\mathcal{L}_{x,C_b}^4) \right. \\ &\quad \left. + \min_{\Gamma_z} (\mathcal{L}_{x,C_g}^4) + \min_{\Gamma_z} (\mathcal{L}_{x,C_r}^4) \right). \end{aligned} \quad (61)$$

Now we calculate the terms  $\mathcal{L}_{x,C_b}^4$ ,  $\mathcal{L}_{x,C_g}^4$ , and  $\mathcal{L}_{x,C_r}^4$  separately as follows:

$$\begin{aligned} \mathcal{L}_{x,C_b}^4 &= \sum_{i \in C_b} \langle [\sigma_{x,i}, Z_1 Z_3 \mathcal{B}_p^z], [\sigma_{x,i}, Z_1 Z_3 \mathcal{B}_p^z] \rangle \\ &= \sum_{i \in C_b} \langle [\sigma_{x,i}, Z_3 \mathcal{B}_p^z], [\sigma_{x,i}, Z_3 \mathcal{B}_p^z] \rangle, \end{aligned} \quad (62)$$

where the second line is the consequence of commutativity of  $Z_1$  with all of  $\sigma_{x,i}$ ,  $i \in C_b$ . In addition, as we proved in the previous case, a lower bound of this quantity is given by Eq. (59) and, by symmetry, it is equal to the lower bound of  $\mathcal{L}_{x,C_g}^4$ . The only term that remains to be obtained is  $\mathcal{L}_{x,C_r}^4$ . One finds that

$$\begin{aligned} \mathcal{L}_{x,C_r}^4 &= \sum_{i \in C_r} \langle [\sigma_{x,i}, Z_1 Z_3 \mathcal{B}_p^z], [\sigma_{x,i}, Z_1 Z_3 \mathcal{B}_p^z] \rangle \\ &= \sum_{i \in C_r} \langle [\sigma_{x,i}, Z_1 \mathcal{B}_p^z], [\sigma_{x,i}, Z_1 \mathcal{B}_p^z] \rangle \\ &= \sum_{i \in C_r} \langle [\sigma_{x,i}, Z_2 Z_g \mathcal{B}_p^z], [\sigma_{x,i}, Z_2 Z_g \mathcal{B}_p^z] \rangle \\ &= \sum_{i \in C_r} \langle [\sigma_{x,i}, \mathcal{B}_p^z], [\sigma_{x,i}, \mathcal{B}_p^z] \rangle, \end{aligned} \quad (63)$$

which is what we discussed in the first case and is equal to the gap of Ising model. Therefore, a lower bound of  $G_4$  is given by

$$G_4 \geq e^{-\beta\Delta} h(\Delta) G_{\text{Ising}}. \quad (64)$$

To obtain the gap of  $\mathcal{L}$  it is enough to consider only the above sectors of the observables, since each of the other sectors is equivalent to one of the four mentioned cases, and this is straightforward to check. Therefore, the minimum of the decay rate in all of the sectors can be obtained by doing minimization only over these four sectors. Finally, we arrive at our key theorem

*Theorem.* The gap of Lindblad superoperator for topological color code due to the coupling to a thermal bath is given by

$$[G(-\mathcal{L})]_{\text{TCC}} \geq e^{-\beta\Delta} h(\Delta) [G(-\mathcal{L})]_{\text{Ising}}. \quad (65)$$

## VI. CONCLUSION

In this work, we have studied thermal stability of the topological color code in the presence of a thermal bath of the form (26). To this end, we have studied the Lindblad evolution of the observables in the Heisenberg picture and their autocorrelation functions. The observables that we studied commute with the Hamiltonian in order to be regarded as logical operators acting on the code space. We obtain a lower bound of the decay rate of these observables as follows:

$$\langle X, X(t) \rangle \leq e^{-\epsilon t} \langle X, X \rangle, \quad (66)$$

where

$$\epsilon \geq e^{-\beta\Delta} h(\Delta) [G(-\mathcal{L})]_{\text{Ising}}, \quad (67)$$

$[G(\mathcal{L})]_{\text{Ising}}$  turns out to be a constant independent of the system size [22], and  $\Delta$  is the gap of the TCC model which is equal

to  $6J$ . Our result means that the autocorrelation function of the observables decreases exponentially in time faster than an exponential with a constant decay rate independent of the system size, i.e., by increasing the system size one cannot decrease the decay rate to make the memory stable. Thus, in a finite time, the autocorrelation function becomes very small and the encoded information will be lost. Therefore, we can conclude that the topological color code is unstable against thermal fluctuations from the bath at finite temperature, even though it is stable at  $T = 0$  against local quantum perturbations.

Although the conclusion about the thermal instability of the color code is the same as that of the Kitaev code, notice however that the derivation of this result is very different in the case of color code from the case of Kitaev model. For example, in Kitaev model excitations appear in pairs as opposed to color code, in which excitations do not appear necessarily in pairs. Moreover, in the Kitaev model, to have all possible excitations, one should apply tensor products of  $\sigma_x$ 's ( $\sigma_z$ 's) over qubits belonging to the subsets of the snake (comb), on the ground states (for further details, see [22]). This is in contrast to the color code where, to have all possible excitations, one should apply a completely different procedure using the concepts of open strings and the branching points as defined in Sec. V A. As explained in Sec. V B, the generators of the observables for any stabilizer Hamiltonian are the stabilizers which are in the Hamiltonian as well as the generators needed for creating all kind of excitations. Apart from the difference of the stabilizers in the two models, because the generators needed for creating all kinds of excitations in the case of color code are different from that of Kitaev, one can conclude that the generators needed to have all observables in the case of color code are different from the Kitaev. The last distinctive point is that the process of creation of the excitations caused by the external bath in the TCC can be mapped to the corresponding process in inhomogeneous one-dimensional Ising model, in contrast to the case of the Kitaev model which can be mapped to the one-dimensional homogeneous Ising model [22].

The impact of these results goes beyond the field of quantum computation and extends to the new emerging field of topological orders in condensed-matter system (strongly correlated spins). In fact, it is known that two-body Hamiltonians in 2D lattices can give rise to topological color codes in the low-energy sector for certain regimes of the couplings [39,40]. These topological orders are expected to suffer from thermal instabilities as well.

#### ACKNOWLEDGMENTS

The author wishes to thank M. A. Martin-Delgado and Markus Müller for fruitful discussions. This work has been done during the author's stay at Complutense University of Madrid and the author wishes to thank the Department of Physics of Complutense University for hospitality and partial financial support. The author also would like to thank V. Karimipour for introducing her to M. A. Martin-Delgado's research group and also reading the manuscript. The author also wishes to thank National Elites Foundation of Iran for partial financial support.

#### APPENDIX: NEGATIVITY OF LINDBLAD SUPEROPERATOR

*Lemma.* The Lindblad superoperator is negative which means that

$$-\langle X, \mathcal{L}(X) \rangle \geq 0, \quad \forall X. \quad (\text{A1})$$

*Proof.* In order to prove the positivity of  $-\langle X, \mathcal{L}(X) \rangle$  we use the definition of  $\mathcal{L}(X)$ :

$$\begin{aligned} -\mathcal{L}(X) &= -\sum_{\alpha} \sum_{\omega \geq 0} \mathcal{L}_{\alpha, \omega}(X) \\ &= \frac{1}{2} \sum_{\alpha} \sum_{\omega \geq 0} h_{\alpha}(\omega) (S_{\alpha}^{\dagger}(\omega) [S_{\alpha}(\omega), X] \\ &\quad + [X, S_{\alpha}^{\dagger}(\omega)] S_{\alpha}(\omega) + e^{-\beta\omega} S_{\alpha}(\omega) [S_{\alpha}^{\dagger}(\omega), X] \\ &\quad + e^{-\beta\omega} [X, S_{\alpha}(\omega)] S_{\alpha}^{\dagger}(\omega)). \end{aligned} \quad (\text{A2})$$

Since  $\frac{1}{2}h_{\alpha}(\omega)$ 's are positive, we prove the positivity of each term  $-\langle X, \mathcal{L}_{\alpha, \omega}(X) \rangle$ :

$$\begin{aligned} -\langle X, \mathcal{L}_{\alpha, \omega}(X) \rangle &= \langle X, S_{\alpha}^{\dagger}(\omega) [S_{\alpha}(\omega), X] + [X, S_{\alpha}^{\dagger}(\omega)] S_{\alpha}(\omega) \\ &\quad + e^{-\beta\omega} \langle X, S_{\alpha}(\omega) [S_{\alpha}^{\dagger}(\omega), X] + [X, S_{\alpha}(\omega)] S_{\alpha}^{\dagger}(\omega) \rangle. \end{aligned} \quad (\text{A3})$$

Expanding the above equation and using the relation  $\rho_{\beta} S_{\alpha}(\omega) = e^{\beta\omega} S_{\alpha}(\omega) \rho_{\beta}$ , one can find that

$$\begin{aligned} -\langle X, \mathcal{L}_{\alpha, \omega}(X) \rangle &= \langle [S_{\alpha}(\omega), X], [S_{\alpha}(\omega), X] \rangle \\ &\quad + e^{-\beta\omega} \langle [S_{\alpha}^{\dagger}(\omega), X], [S_{\alpha}^{\dagger}(\omega), X] \rangle. \end{aligned} \quad (\text{A4})$$

In order to prove the positivity of  $\langle [S_{\alpha}(\omega), X], [S_{\alpha}(\omega), X] \rangle$  one needs to use the explicit form of  $S_{\alpha}(\omega)$ , which for  $x$  type errors is as follows.

(i) *Annihilation of three excitations.* If there are three excitations in the three plaquettes that have this qubit in common,  $\sigma_{x,i}$  annihilates all of them [Fig. 4(a)]. Thus the Fourier transform of  $\sigma_{x,i}$  is given by

$$\begin{aligned} S_{x,i}(\omega = 6J) &= \Pi_{-3J} \sigma_{x,i} \Pi_{3J} \\ &= \frac{1}{8} \sigma_{x,i} (1 - B_p^z) (1 - B_{p'}^z) (1 - B_{p''}^z). \end{aligned} \quad (\text{A5})$$

Here,  $p$ ,  $p'$ , and  $p''$  are the three plaquettes that have the  $i$ th qubit in common,  $\Pi_{3J}$  denotes the projector onto the subspace with three excitations, and  $\Pi_{-3J}$  denotes the projector onto the subspace with no excitation in these three plaquettes.

(ii) *Creation of one excitation and annihilation of two.* If there are two excitations in two of the plaquettes that have this qubit in common,  $\sigma_{x,i}$  annihilates them and creates one excitation in the other plaquette [Fig. 4(b)]. Thus the Fourier transform of  $\sigma_{x,i}$  is given by

$$\begin{aligned} S_{x,i}(\omega = 2J) &= \Pi_{-J} \sigma_{x,i} \Pi_J \\ &= \frac{1}{8} \sigma_{x,i} ((1 - B_p^z) (1 - B_{p'}^z) (1 + B_{p''}^z) \\ &\quad + (1 - B_p^z) (1 + B_{p'}^z) (1 - B_{p''}^z) \\ &\quad + (1 + B_p^z) (1 - B_{p'}^z) (1 - B_{p''}^z)). \end{aligned} \quad (\text{A6})$$

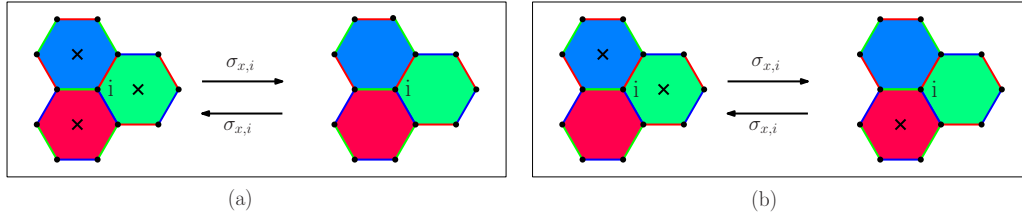


FIG. 4. Two possibilities of creation and annihilation of excitations in TCC due to existence of a thermal bath. (a) Creation and annihilation of three excitations. (b) Creation of one excitation and annihilation of two, and vice versa.

Here,  $\Pi_J$  denotes the projector onto the subspace with two excitations and  $\Pi_{-J}$  denotes the projector onto the subspace with one excitation.

Therefore, we have

$$\begin{aligned} S_{x,i}(6J) &= \sigma_{x,i} \Pi_{3J}, & S_{x,i}^\dagger(6J) &= \sigma_{x,i} \Pi_{-3J}, \\ S_{x,i}(2J) &= \sigma_{x,i} \Pi_J, & S_{x,i}^\dagger(2J) &= \sigma_{x,i} \Pi_{-J}. \end{aligned} \quad (\text{A7})$$

All of the above arguments can be done in a similar fashion for the  $z$  type error by substituting  $\sigma_{z,i}$  for  $\sigma_{x,i}$  and  $B_p^x$  for  $B_p^z$ .

It is sufficient to prove the positivity of  $\langle [S_\alpha(\omega), X], [S_\alpha(\omega), X] \rangle$  for a specific  $\omega$ , say  $6J$ . For the other  $\omega$ 's the procedure is the same. For this case  $\langle [S_\alpha(\omega), X], [S_\alpha(\omega), X] \rangle$  is equal to the following:

$$\begin{aligned} &\text{tr}(\rho_\beta \Pi_{3J} [X, \sigma_{x,i}] [\sigma_{x,i}, X] \Pi_{3J}) \\ &= \text{tr} \left( \Pi_{3J} \rho_\beta \underbrace{[X, \sigma_{x,i}]}_{A^\dagger} \underbrace{[\sigma_{x,i}, X]}_A \right). \end{aligned} \quad (\text{A8})$$

Since  $\Pi_{3J}$  is a projector onto a subspace of the system's Hilbert space it can be written as

$$\Pi_{3J} = \sum_m |\Psi_m\rangle \langle \Psi_m|. \quad (\text{A9})$$

The thermal state ( $\rho_\beta$ ) also can be written as a mixture of eigenstates of the Hamiltonian, i.e.,

$$\rho_\beta = \sum_k \lambda_k |\Psi_k\rangle \langle \Psi_k|. \quad (\text{A10})$$

Therefore, we have

$$\Pi_{3J} \rho_\beta = \sum_m \lambda_m |\Psi_m\rangle \langle \Psi_m|. \quad (\text{A11})$$

If we diagonalize matrix  $A$  and expand the eigenstates of the Hamiltonian as a superposition of the eigenstates of  $A$ , i.e.,

$$|\Psi_m\rangle = \sum_a \psi_{m,a} |\Psi_{m,a}\rangle, \quad (\text{A12})$$

we will end in the following:

$$\text{tr}(\rho_\beta \Pi_{3J} [X, \sigma_{x,i}] [\sigma_{x,i}, X] \Pi_{3J}) = \sum_{m,a} \lambda_m |\psi_{m,a}|^2, \quad (\text{A13})$$

which is clearly positive.

These arguments are not particular for TCC. For the other models  $\omega$ 's and  $\Pi$ 's are different; nevertheless, the procedure of the proof is the same as above.

- 
- [1] P. W. Shor, Scheme for reducing decoherence in quantum computer memory, *Phys. Rev. A* **52**, R2493(R) (1995).
- [2] A. M. Steane, Error Correcting Codes in Quantum Theory, *Phys. Rev. Lett.* **77**, 793 (1996).
- [3] D. Gottesman, A class of quantum error-correcting codes saturating the quantum Hamming bound, *Phys. Rev. A* **54**, 1862 (1996).
- [4] A. R. Calderbank and P. W. Shor, Good quantum error-correcting codes exist, *Phys. Rev. A* **54**, 1098 (1996).
- [5] A. Yu Kitaev, Quantum computations: Algorithms and error correction, *Russ. Math. Surv.* **52**, 1191 (1997).
- [6] A. R. Calderbank, E. M. Rains, P. M. Shor, and N. J. A. Sloane, Quantum Error Correction and Orthogonal Geometry, *Phys. Rev. Lett.* **78**, 405 (1997).
- [7] J. Preskill, Reliable quantum computers, *Proc. R. Soc. A: Math., Phys. Eng. Sci.* **454**, 385 (1998).
- [8] D. Gottesman, Fault-tolerant quantum computation with higher-dimensional systems, in *Quantum Computing and Quantum Communications* (Springer, Berlin, 1999), pp. 302–313.
- [9] D. Gottesman, An introduction to quantum error correction and fault-tolerant quantum computation, *Proc. Symp. Appl. Math.* **68**, 13 (2009).
- [10] J. Preskill, Lecture Notes in Quantum Computation, <http://www.theory.caltech.edu/people/preskill/ph229/notes/chap7.pdf>.
- [11] B. M. Terhal, Quantum error correction for quantum memories, *Rev. Mod. Phys.* **87**, 307 (2015).
- [12] A. Y. Kitaev, Fault-tolerant quantum computation by anyons, *Ann. Phys. (N.Y.)* **303**, 2 (2003).
- [13] H. Bombin and M. A. Martin-Delgado, Topological Quantum Distillation, *Phys. Rev. Lett.* **97**, 180501 (2006).
- [14] E. Dennis, A. Kitaev, A. Landahl, and J. Preskill, Topological quantum memory, *J. Math. Phys.* **43**, 4452 (2002).
- [15] H. G. Katzgraber, H. Bombin, and M. A. Martin-Delgado, Error Threshold for Color Codes and Random Three-Body Ising Models, *Phys. Rev. Lett.* **103**, 090501 (2009).
- [16] R. S. Andrist, H. G. Katzgraber, H. Bombin, and M. A. Martin-Delgado, Tricolored lattice gauge theory with randomness: Fault tolerance in topological color codes, *New J. Phys.* **13**, 083006 (2011).
- [17] H. Bombin, R. S. Andrist, M. Ohzeki, H. G. Katzgraber, and M. A. Martin-Delgado, Strong Resilience of Topological Codes to Depolarization, *Phys. Rev. X* **2**, 021004 (2012).

- [18] T. Ohno, G. Arakawa, I. Ichinose, and T. Matsui, Phase structure of the random-plaquette  $Z_2$  gauge model: Accuracy threshold for a toric quantum memory, *Nucl. Phys. B* **697**, 462 (2004).
- [19] H. Bombin and M. A. Martin-Delgado, Topological Computation Without Braiding, *Phys. Rev. Lett.* **98**, 160502 (2007).
- [20] D. Nigg, M. Muller, E. A. Martinez, P. Schindler, M. Hennrich, T. Monz, M. A. Martin-Delgado, and R. Blatt, Quantum computations on a topologically encoded qubit, *Science* **345**, 302 (2014).
- [21] R. Alicki, M. Fannes, and M. Horodecki, A statistical mechanics view on Kitaev's proposal for quantum memories, *J. Phys. A: Math. Theor.* **40**, 6451 (2007).
- [22] R. Alicki, M. Fannes, and M. Horodecki, On thermalization in Kitaev's 2D model, *J. Phys. A: Math. Theor.* **42**, 065303 (2009).
- [23] R. Alicki, M. Horodecki, P. Horodecki, and R. Horodecki, On thermal stability of topological qubit in Kitaev's 4D model, *Open Syst. Inf. Dyn.* **17**, 1 (2010).
- [24] H. Bombin, R. W. Chhajlany, M. Horodecki, and M. A. Martin-Delgado, Self-correcting quantum computers, *New J. Phys.* **15**, 055023 (2013).
- [25] A. Kubica, B. Yoshida, and F. Pastawski, Unfolding the color code, *New J. Phys.* **17**, 083026 (2015).
- [26] H. Bombin and M. A. Martin-Delgado, Exact topological quantum order in  $D=3$  and beyond: Branyons and brane-net condensates, *Phys. Rev. B* **75**, 075103 (2007).
- [27] We denote the red plaquettes by R, the green plaquettes by G, and the blue plaquettes by B.
- [28] A stabilizer is an operator which acts as identity in the code space.
- [29] C. Cafaro and P. van Loock, Approximate quantum error correction for generalized amplitude-damping errors, *Phys. Rev. A* **89**, 022316 (2014).
- [30] C. Cafaro and S. Mancini, Quantum stabilizer codes for correlated and asymmetric depolarizing errors, *Phys. Rev. A* **82**, 012306 (2010).
- [31] A. Rivas and S. F. Huelga, *Open Quantum Systems. An Introduction* (Springer, Heidelberg, 2011).
- [32] E. B. Davies, Markovian master equations, *Commun. Math. Phys.* **39**, 91 (1974).
- [33] R. Alicki and L. Lendi, *Quantum Dynamical Semigroups and Applications* (Springer, Berlin, 2007).
- [34] H. P. Breuer and F. Petruccione, *The Theory of Open Quantum Systems* (Oxford University Press, Oxford, 2002).
- [35] R. Alicki and M. Fannes, Decay of fidelity in terms of correlation functions, *Phys. Rev. A* **79**, 012316 (2009).
- [36] One should note that the red links have three distinct orientations as shown in Fig. 1, but only the links with one specific orientation are sufficient here.
- [37] In order for the generators to commute with each other we take two distinct branching points for the two types  $x$  and  $z$ . The branching points are shown as  $b_x$  and  $b_z$  in Fig. 2(b).
- [38]  $Z_i$  and  $X_i$  operators are defined on the nontrivial loops shown in Fig. 1(b).
- [39] H. Bombin, M. Kargarian, and M. A. Martin-Delgado, Interacting anyonic fermions in a two-body color code model, *Phys. Rev. B* **80**, 075111 (2009).
- [40] M. Kargarian, H. Bombin, and M. A. Martin-Delgado, Topological color codes and two-body quantum lattice Hamiltonians, *New J. Phys.* **12**, 025018 (2010).